The Role of Subsurface Flow in Hillslope and Stream Bank Erosion: A Review

Garey A. Fox*

Dep. of Biosystems and Agric. Eng.
Oklahoma State Univ.
Stillwater, OK 74078

G. V. Wilson

USDA-ARS
National Sedimentation Lab.
598 McElroy Dr.
Oxford, MS 38655

Sediment is one of the most common causes of stream impairment. Great progress has been made in understanding the processes of soil erosion due to surface runoff and incorporating these in prediction technologies. In many landscapes, however, the dominant source of sediment is derived from mass wasting of hillslopes and stream banks, potentially driven by subsurface flow. We highlight the mechanisms and importance of subsurface flow processes in erosion associated with hillslopes and stream banks. Subsurface flow affects erosion directly by seepage and pipe flow processes and indirectly by the relationship of soil properties with soil water pressure. Seepage contributes to erosion through interrelated mechanisms: hydraulic gradient forces that reduce the resistance of the particle to dislodging from the soil matrix and particle mobilization when soil particles become entrained in exfiltrating water. Preferential flow through soil pipes results in internal erosion of the pipe, which may produce gullies by tunnel collapse. The eroded material can clog soil pipes, causing pore water pressure buildup inside the pipes that can result in landslides, debris flows, embankment failures, or reestablishment of ephemeral gullies. Research in the past decades has advanced our understanding of these processes, leading to mathematical relationships that can be incorporated into mechanistic, process-based models. Further research advances are necessary, however, especially on the complexity of the interactive effects of surface flow, seepage, pipe flow, and vegetation on soil erosion properties. More information is needed on the extent that subsurface flow contributes to hillslope and stream bank erosion. We believe that multidisciplinary efforts between soil scientists, geotechnical engineers, hydraulic engineers, and hydrologists are necessary to fully understand and integrate subsurface flow and soil erosion processes in simulation tools.

Sediment has been listed as one of the most common causes of stream impairment in the United States (USEPA, 2000). In many areas, the dominant source of sediment is the stream bank itself. Mass failure of stream banks can contribute up to 85% of the sediment yield (Simon and Darby, 1999). Wilson et al. (2008a) used radionuclide tracers in five agricultural watersheds to determine that between 54 and 80% of the stream sediment was derived from the stream bank. In steep terrains, hillslope failures, such as landslides and debris flows, are the predominant process of landscape evolution (Iida, 2004) and are a significant, if not dominant, source of sediment to streams (Gomi et al., 2004). For more gentle slopes, gully erosion, which is a form of hillslope failure, can be a significant source of stream sediment. Poesen et al. (2003) estimated that, on average, 44% of the total soil erosion worldwide was by gullies, whereas the NRCS (1997) estimated that 35% of the total soil loss was by gully erosion in the United States. Historically the emphasis of erosion research has been on sheet and rill erosion, with the hydrologic focus on surface flow processes. Consideration for subsurface flow contributions to these erosion processes has largely been neglected in assessments and prediction technologies due to the lack of experimental observations and insufficient understanding of the governing processes.

It is often hypothesized that subsurface flow is contributing to bank or hillslope instability, such as the massive stream bank failure in 2007 along the Danube

---

River in Hungary (Ujvari et al., 2009) or the fatal landslides that occurred in 2003 in Japan (Sidle and Chigira, 2004). The tools, however, are either not available or inadequate to measure or model subsurface flow to definitively associate its role in the failure event. Geomorphologists have historically recognized the role of seepage in erosion processes and used amphitheater-shaped canyons as a diagnostic indicator of erosion by seepage (Lamb et al., 2007, 2008). Such features on Mars have been used to suggest seepage as the governing erosion mechanism for Martian valley networks (Luo and Howard, 2008). A number of recent field, laboratory, and modeling investigations (Fig. 1 and 2) have highlighted the role of subsurface flow in stream bank failure (Wilson et al., 2007; Fox et al., 2006, 2007; LaSage et al., 2008; van Balen et al., 2008) and landslides (Onda et al., 2004).

A common feature often associated with subsurface flow contributing to hillslope and stream bank failure is the occurrence of a water-restricting layer that perches water, sometimes termed a *duplex soil* (Faulkner, 2006). Hillslope failures attrib-

uted to subsurface flow are often associated with shallow soils over bedrock (Onda et al., 2004; Sidle et. al., 2006). Vieira and Fernandes (2004) noted that landslide scars in the notoriously unstable Rio de Janeiro, Brazil, region typically occur at the boundary of soil and bedrock. They observed a difference of two orders of magnitude in the saturated hydraulic conductivity, K_s, between such layers, which they concluded could result in localized high pore water pressures sufficient to trigger landslides. Stream bank failures by subsurface flow may not be associated with shallow soils over bedrock but simply the occurrence of conductive layers residing over less permeable layers. Wilson et al. (2007) noted that a 16% increase in clay content between stream bank layers resulted in a decrease in K_s of two and a half orders of magnitude. These thin (around 10 cm) contrasting layers were associated with seep locations. Fox et al. (2007) noted that differences of less than an order of magnitude in vertical K_s between stream bank layers may be sufficient to cause lateral flow, resulting in stream bank instability due to anisotropy of the
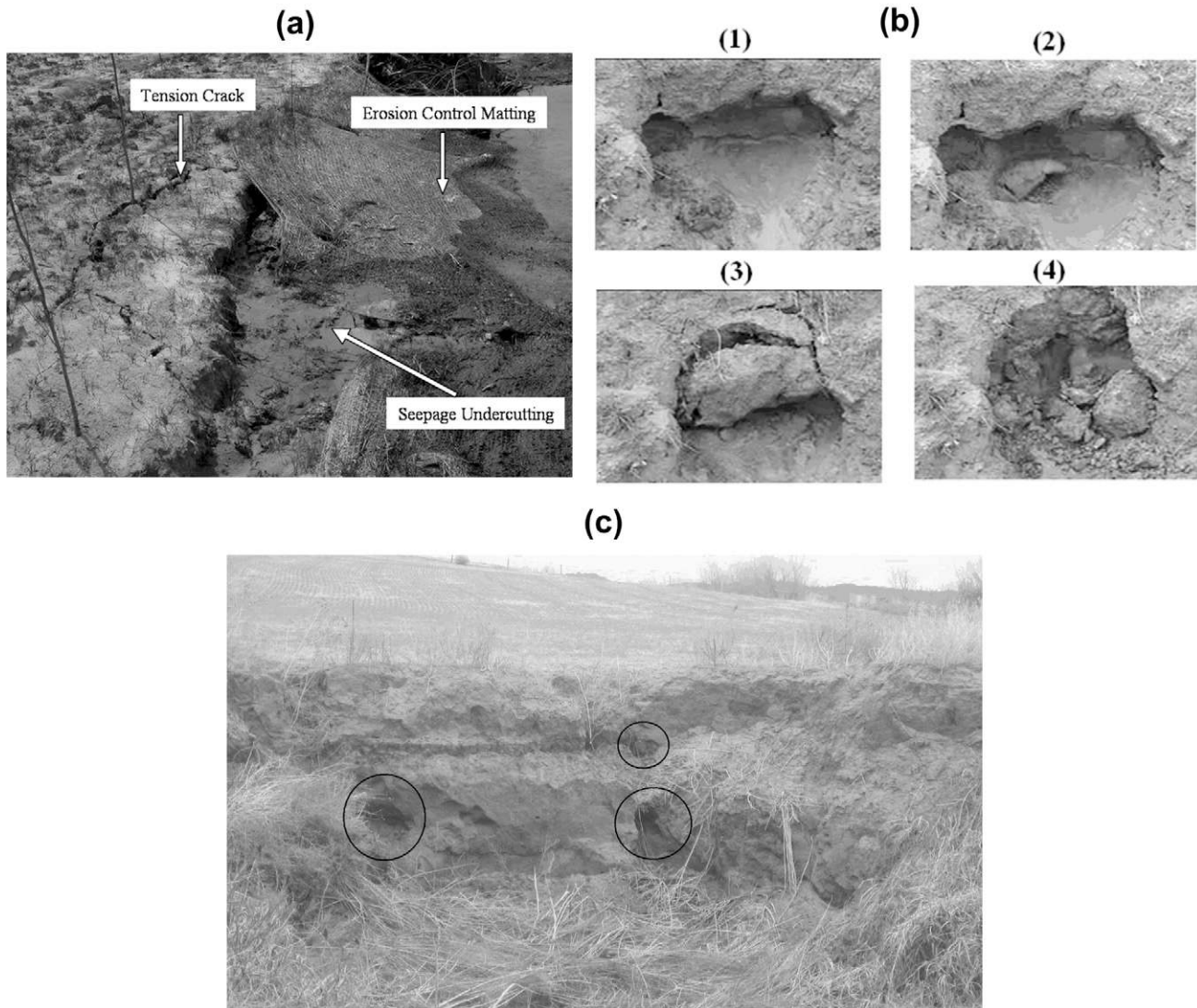

Fig. 1. Examples of seepage erosion undercutting and sapping at three field sites in the United States: (a) a stream restoration project in eastern North Carolina undermined by sapping failure (from Lindow et al. [2009], with permission from John Wiley & Sons, Ltd.); (b) time series of seepage erosion undercut formation in sloughed bank material at Goodwin Creek in northeastern Mississippi (modified from Fox et al. [2007], with permission from John Wiley & Sons, Ltd.); and (c) seepage erosion undercuts along a Sugar Creek stream bank in southwestern Oklahoma.

conductive layer above the restrictive layer. Such a soil profile is typical of the alluvial process that creates stream banks in which multiple deposition events result in alternating layers of coarse-grained material over finer grained layers. Shallow soils over bedrock are also typical of steep hillslopes. Thus, seepage should be considered a possible instability mechanism rather than neglecting the impact of such forces on hillslopes and stream banks, particularly in humid regions with restrictive sublayers.

Seepage from stream banks can lead to erosion and mass failure through several interrelated mechanisms: pore water pressure effects on soil shear stress, hydraulic gradient forces acting on the bank, and mobilization of particles in the seepage flow (Fig. 1 and 2). According to Dunne (1990), erosion by seepage can occur as fluid particulate transport or mass failure. The former occurs when the fluid stresses cause soil particles to become entrained in the seepage, whereas mass failure occurs when the driving forces acting on a soil mass exceed the resisting forces. Both mechanisms are often termed *sapping*, but we distinguish here *seepage erosion* as specifically the transport of particles entrained in seepage flow and *sapping* as the mass failure that can result from seepage forces, seepage erosion, or other processes.

One subsurface flow process that has garnered considerably less attention than seepage with regard to slope or bank stability has been preferential flow through soil pipes. Soil pipes tend to develop in duplex soils above water-restricting horizons and are basically the same as macropores but are generally taken to occur parallel to the slope and be of sufficient length, size, and connectivity to influence flow at the hillslope scale (Uchida et al., 2001; Faulkner, 2006). The term *piping* is often used to refer to the combined or indistinguishable effects of seepage and flow through a discrete soil pipe (Dunne, 1990; Bryan and Jones, 1997). Hydraulic and geotechnical engineers conventionally refer to seepage below an earthen embankment as piping. A clear distinction can be made, however, between piping by seepage and flow through a soil pipe due to differences in their hydraulic and erosion mechanisms (Kosugi et al., 2004; Wilson et al., 2008b; Wilson, 2009). Both forms of piping involve subsurface flow through a preferential flow path but here, piping or pipe-flow erosion will refer strictly to erosion by flow through a discrete soil pipe.

It is well established that pipe flow, e.g., macropore flow, contributes to streamflow generation in forested hillslopes (Wilson et al., 1990, 1991a,b; McDonnell, 1990; Sidle et al., 2000, Uchida et al., 2001, 2002), even under semiarid conditions (Newman et al., 2004). It has been postulated that this rapid flow through soil pipes is a major cause of landslides and debris flow on hillslopes (Uchida et al., 2001). This can occur when the concentration of flow into soil pipes exceeds their transport capacity or when blockage of the soil pipe by eroded material causes a buildup of internal water pressures in the soil pipe. It is also well established that pipe flow is critical to levee and dam failures. Foster et al. (2000, 2002, p. 75–82) concluded that internal erosion of soil pipes by pipe flow was the leading cause of embankment failures.

Classic gully erosion has been attributed to pipe flow, particularly in Europe, although considerably less attention has been paid to the role of pipe flow in ephemeral gully erosion. Bocco (1991) concluded that 60% of the gullies in European fields were the result of soil piping. Faulkner (2006) provided an excellent review on the role of soil piping in gully erosion and reported that gullies may form at advanced stages of development when soil pipes erode to the extent that tunnel collapse occurs. Faulkner (2006) noted that such gully erosion is usually associated with
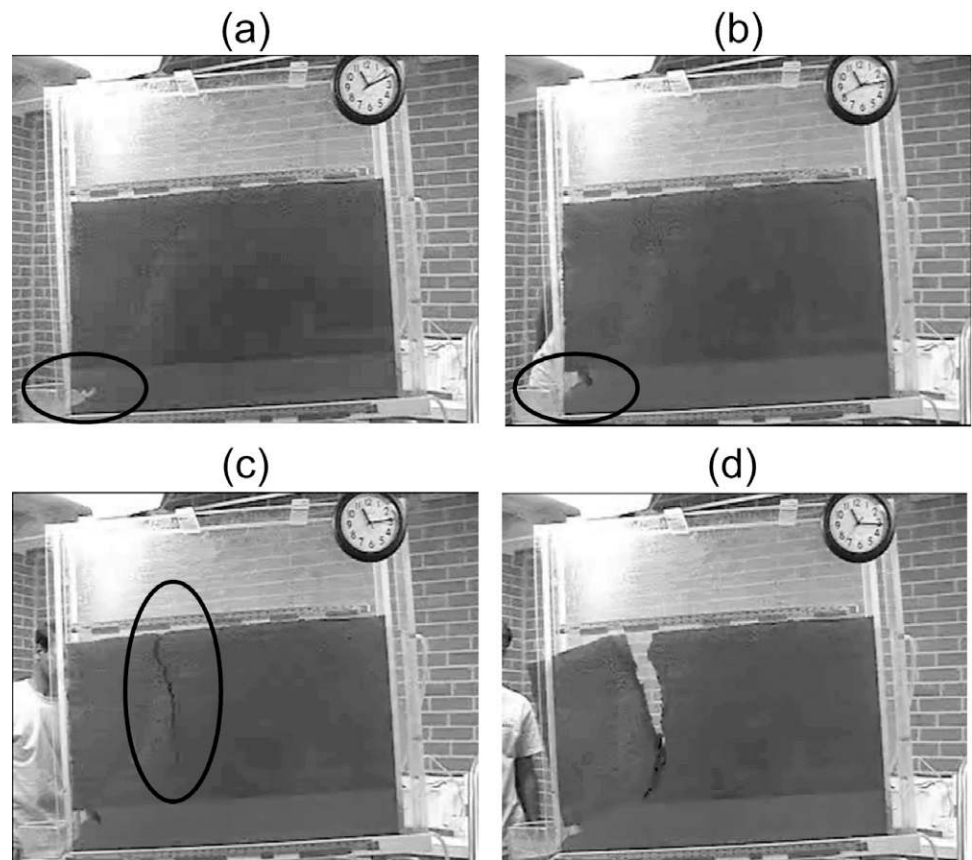

Fig. 2. Two-dimensional seepage and sapping experiments performed by Fox et al. (2006) demonstrating a typical time series of simulated Little Topashaw Creek bank failure due to seepage erosion in two-dimensional lysimeter experiments: (a) seepage erosion undercutting, (b) undermining, (c) tension crack formation, and (d) bank collapse (sapping). The Little Topashaw Creek stream banks consist of alternating layers of silt loam, loamy sand, and silt with a conductivity contrast of two orders of magnitude. (Source: Fox et al. [2006], with permission from the American Society of Civil Engineers (ASCE). This material may be downloaded for personal use only. Any other use requires prior permission of the ASCE).

duplex soils in which the soil pipe forms immediately above the water-restricting layer. Ephemeral gullies formed by soil piping produce soil pipes that are no longer continuous in the landscape but are cut off when the ephemeral gully is filled in by tillage.

Wilson et al. (2008b) conducted laboratory studies using a 2-cm-i.d. soil pipe, immediately above an impermeable layer, that was connected to a constant-head reservoir and extended 50 cm into a 150-cm soil bed. They showed that flow into discontinuous soil pipes, when synergistically combined with rainfall, cause sudden pop-out failures of the hillslope and reformation of the ephemeral gully. Despite the substantial body of work on preferential flow through soils and the many reviews on the subject (Gerke, 2006; Jarvis, 2007), little has been published in the soil science literature on the subject of pipe flow related to stream bank failure or gully erosion.

The objective of this review is to describe and document the current state of the science of subsurface flow mechanisms (i.e., increased soil pore-water pressure effects, hydraulic gradient forces, seepage erosion by particle mobilization, and soil piping) related to stream bank and hillslope instability. This review also outlines future research needs, especially improved process-based modeling that considers seepage and soil piping mechanisms of erosion on bank instability, and highlights the importance of soil scientists and engineers getting more involved in this area of research.

SEEPAGE MECHANISMS OF SLOPE INSTABILITY
Soil Pore-Water Pressure Effects on Slope Stability

In unsaturated soils, increasing matrix suction has the effect of increasing the shear strength, s, of the soil, as described by Fredlund and Rahardjo (1993) and Fredlund and Vanapalli (2002):

$$s=\left[c'+\left(\sigma_n-u_w\right)\tan\phi'\right]+\left[\left(u_a-u_w\right)\tan\phi^b\right] \qquad [1]$$

where c' is the effective cohesion of the soil, u_a and u_w are the pore-air and -water pressures, respectively, such that their difference $(u_a - u_w)$ is the matrix suction (negative pressure head) (all variables are defined in the Appendix). The difference between the total normal stress, σ_n, and u_w is the net normal stress, ϕ' is the angle of internal friction, and ϕ^b is the angle indicating the rate of increase in the shear strength relative to matrix suction and is generally between 10 and 20° (Fredlund and Rahardjo, 1993; Simon et al., 1999). For saturated soil, the matrix suction is zero and thus the saturated shear strength is represented by the term in the first brackets of the equation.

The removal of negative soil pore-water pressures, reducing the shear strength, s, of the soil, has been discussed in detail by Rinaldi and Casagli (1999), Simon et al. (1999), and Darby et al. (2007). The importance of this instability mechanism has led to work by Darby et al. (2007) and Rinaldi et al. (2008) in linking subsurface flow, fluvial (streamflow) hydraulics, and stream bank stability models. The commonly observed bank failure on the recession limb of hydrographs has been attributed to the interrelated combination of the increase in pressure head, due to both vertical infiltration through the soil surface and lateral infiltra-

tion through the bank face from the stream during high stage, and reduced confining pressure as the stream stage decreases. As discussed below, however, there are other processes besides return flow of bank storage that may be causing bank failures during the recession limb of hydrographs.

Seepage Gradient Forces Effects on Slope Stability

Groundwater seepage exerts forces (SF, force per unit volume) on bank sediment proportional to the hydraulic gradient, $\partial h/\partial y$:

$$\text{SF}=\rho g\frac{\partial h}{\partial y} \qquad [2]$$

where ρ is the density of the fluid, g is gravity, h is the hydraulic head, and y is the distance (Lobkovsky et al., 2004; Ghiassian and Ghareh, 2008). When isolated, hydraulic gradient forces can lead to Coulomb mass failure or liquefaction of the soil mass when upward seepage forces become equivalent to the submerged weight of the sediment (Iverson and Major, 1986; Ghiassian and Ghareh, 2008). In terms of Coulomb failures, Chu-Agor et al. (2008a) demonstrated in laboratory experiments that such gradients can lead to failures with little indication of the presence of groundwater instability. These types of failures generally occur on banks with low initial resistive strength (i.e., noncohesive or low-bulk-density soils). The stream restoration project reported by Lindow et al. (2009) was undermined due to bank collapses hypothesized to be due to seepage gradient forces (Fig. 1). Lindow et al. (2009) observed in two-dimensional lysimeter experiments with a repacked bank (10 cm of sand at bulk density ρ_b = 1.30 Mg m^{-3} underlying 15 cm of sandy clay loam) that sliding failures of underlying bank layers eventually led to undermining of the entire bank.

Frequently, mass failure analysis evaluates the balance of forces acting on a soil element, typically assuming noncohesive soils and an infinite slope. It attempts to predict the conditions whereby the resultant of the driving forces exceeds the resultant of the stabilizing forces, causing small or large masses of soil to fail. For example, an infinite slope approach or analysis was used by Budhu and Gobin (1996) to analyze the minimum, stable seepage-slope angle for an infinite, noncohesive slope under a steady-state seepage regime. Their study showed that in order for liquefaction to occur, the vertical component of the seepage force must be equal to or greater than the weight of the soil. The seepage-slope angle relationship was given as

$$\left(\cos\alpha'+\cos\lambda\right)\frac{\sin\alpha'}{\sin\lambda}=\frac{\gamma_{\text{sat}}}{\gamma_w}$$
$$=\frac{G-1}{1+e} \qquad [3]$$
$$=(1-n)(G-1)$$

where λ is the direction of the seepage vector measured clockwise from the inward normal to the bank slope (α'), γ_{sat} is the saturated weight of the soil, γ_w is the unit weight of water, G is the specific gravity of the soil, e is the void ratio, and n is the soil

porosity. Their results showed that for most soils, static liquefaction occurs when the seepage is directed vertically upward.

The critical conditions necessary for sapping, i.e., seepage resulting in mass failure of banks, can be evaluated using a balance of forces acting on a volume of soil. For cohesive soils, sapping results from the weakening of cohesive bonds by weathering, gravity, or other forces near the seepage face (Dunne, 1990). Failure occurs when the critical depth is

$$\Delta z = \frac{c}{i\rho g - (\rho_s - \rho)g(1-n)} \qquad [4]$$

where i is the gradient, ρ_s is the sediment density, Δz is the depth from the surface to where mobilization occurred, and c is the apparent cohesion. Dunne (1990) pointed out the difficulty in using this equation: if c is large, realistic values of the seepage gradient lead to unrealistically thick failed layers, and the seepage gradient has to become unrealistically large to result in liquefaction at the scale of soil fragments that commonly flow by seepage.

Iida (2004) developed a relationship that describes the critical depth of saturated soil, H_{cr}, that can trigger shallow landslides by groundwater flow:

$$H_{cr} = \frac{c - \gamma_w \cos^2\alpha' (\tan\alpha' - \tan\phi')D}{\cos^2\alpha' \left[(\gamma_{sat} - \gamma_{uns})(\tan\alpha' - \tan\phi') + \gamma_w \tan\phi'\right]} \qquad [5]$$

where γ_{uns} is the weight of unsaturated soil and D is the soil depth to bedrock. From this relationship, they computed a probability for a shallow landslide occurring due to perching of water over a restrictive layer, i.e., the probability that the saturated depth exceeds H_{cr}.

Chu-Agor et al. (2008a) investigated tension or "pop-out" failure due to the seepage force exceeding the soil strength by computing the factor of safety of cohesive slopes. They derived the factor of safety (FS) along a failure plane parallel to the bank face as

$$FS = \frac{(c'/z\gamma_w) + \left[(\gamma_{sat}/\gamma_w)\cos\alpha' - \sin\alpha'\cos\lambda\right]\tan\phi'}{\left[(\gamma_{sat}/\gamma_w) + 1\right]\sin\alpha'} \qquad [6]$$

Similarly, FS along a failure plane perpendicular to the bank face is

$$FS = \frac{(c'/b\gamma_w) + \left[(\gamma_{sat}/\gamma_w) + 1\right]\sin\alpha'\tan\phi'}{\sin\alpha'\cot\lambda - (\gamma_{sat}/\gamma_w)\cos\alpha'} \qquad [7]$$

where b and z are the dimensions of the soil block (Fig. 3). In their experiments conducted on a three-dimensional soil block (Fig. 4), tension or "pop-out" failure occurred when the computed FS was <1. When the resistive strength of the bank was greater than the seepage gradient and weight forces, an additional mechanism of stability was required for failure (Fig. 5).

Seepage Erosion Effects on Slope Stability

The third mechanism is instability due to undercutting when seepage exfiltrates the bank and liquefies the soil at the exfiltration point (Fig. 1, Supplemental Video 1: Goodwin Creek seepage erosion and bank sloughing). The transport of soil particles out of the stream bank by seepage produces an undercut in the bank face. This failure mechanism, termed *seepage erosion undercutting*, has been reported in field studies by Hagerty (1991), Fox et al. (2007), and Wilson et al. (2007). This form of undercutting of the stream bank is distinctly different from the undercutting of banks more commonly attributed to fluvial erosion (Simon et al., 2009). These mechanisms of undercutting can be distinguished when the void occurs at an elevation above the stream stage or when it occurs during the hydrograph recession limb after the stream stage has lowered. While similar, the mechanisms creating these are different and thus their impact on bank failure can be distinctly different.

Several recent studies have reported seepage flow and erosion measurements in situ and quantified soil properties associated with seepage erosion. Wilson et al. (2007) and Fox et al. (2007) developed experimental techniques for measuring seepage erosion in situ using 50-cm-wide miniflumes. Seepage flows and sediment
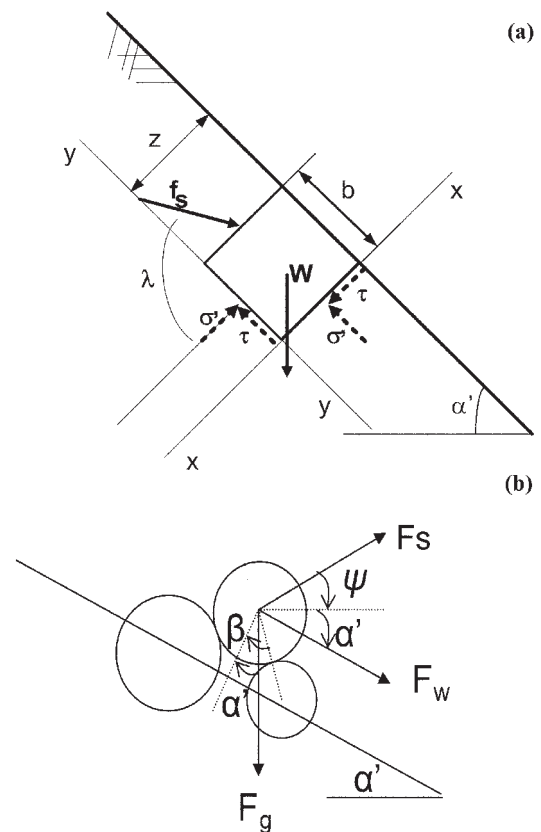

Fig. 3. (a) Free-body diagram of a soil element subjected to seepage force considering two possible failure planes, *yy* and *xx*, as used by Chu-Agor et al. (2008a). The soil element has dimensions *z* and *b* and is subjected to seepage (f_s) and gravity (*W*) forces. (b) Force balance on a particle on a bank inclined at an angle α'. The particle makes an angle β with another particle and is subjected to a seepage force (F_s) exiting the bank at an angle Ψ, a tractive force due to surface runoff (F_w), and gravity (F_g) (after Howard and McLane, 1988). From Chu-Agor et al. (2009), with permission from Elsevier.

concentrations were measured at seep locations on two different streams in Mississippi: Little Topashaw Creek (LTC) and Goodwin Creek (GC). Flow and sediment were allowed to flow through the pan until reaching near-steady-state conditions, and then time-discrete samples were acquired in 0.5- to 1.0-L collection bottles. The flow rate, sediment transport rate, and sediment concentrations were quantified for each sample.

Seepage was measured by Wilson et al. (2007) at eight locations along an 800-m reach of LTC. All but two of the seeps were classified as seepage erosion of a conductive layer overlying a water-restrictive layer. Seepage flow rates ranged from 4 to 931 L d^{-1} and sediment concentrations ranged from 0.4 to 660 g L^{-1}. Wilson et al. (2007) noted that while seepage flows lasted for several days following rainfall events, the flow rates reported were conservative in that measurements could not be made during or immediately after storms.

Most of the seeps at GC (Fox et al., 2007) were classified as undercutting the layers underneath the seepage layer. Seep flow rates averaged 0.39 L min^{-1}, with a maximum of 1.02 L min^{-1}; seepage erosion rates at GC averaged 16.0 g min^{-1}, with a maximum of 68.0 g min^{-1} (Fig. 6). One of the monitored seeps was buried by sloughed bank material from previous bank failures; this seep had an average flow rate of 0.75 L min^{-1} (maximum of

0.84 L min^{-1}) with average sediment transport rates and sediment concentrations of 738 g min^{-1} and 989 g L^{-1}, respectively.

Because of the treacherous nature of measuring seepage in situ, two-dimensional soil lysimeter experiments (see an example in Fig. 2) were conducted to experimentally simulate the soil and hydrologic conditions observed in situ at LTC and GC, in which seepage erosion resulted in stream bank failure without the stream stage contributing to bank storage or failure. These experiments characterized seepage erosion processes in the laboratory using 0.15-m-wide by 1.0-m-long lysimeters with soil packed to the measured bulk density of the stream bank layers, i.e., 0.3 m of topsoil, 0.1 m of conductive layer, and 0.05 m of water-restricting layer. The banks were inclined to different slopes and constant pressure heads up to 30 cm. Wilson et al. (2007) noted that seepage occurred within minutes of head establishment, during which time tensiometers 5 cm above the water-restricting layer had not indicated a response. Thus, seepage may occur with perched water <5 cm above the restrictive layer.

Fox et al. (2006) extended this experimental setup to include topsoil bank materials at various heights up to 80 cm and pressure heads up to 80 cm (Fig. 2). Their two-dimensional laboratory experiments demonstrated the mechanisms of seepage erosion, including seepage erosion undercutting (Fig. 2a), undermining (Fig. 2b), tension crack formation (Fig. 2c), and ultimately bank failure (Fig. 2d) (Supplemental Video 2: Two-dimensional lysimeter experiments of seepage erosion and bank collapse). Such experiments demonstrated fairly rapid bank failures due to small seepage undercuts independent of fluvial forces. Chu-Agor et al. (2008b) numerically modeled these two-dimensional lysimeter experiments using SEEP-W/SLOPE-W and demonstrated through stability modeling that small degrees of undercutting by seepage erosion can exponentially reduce stream bank stability (Fig. 7); however, this modeling was predicated on having observations of seepage undercut distances for incorporation into the simulation domain.

Several equations have been proposed for predicting the initiation of particle mobilization by seepage, primarily for noncohesive soils. Such equations attempt to predict the limiting conditions when the seepage force across the grain exceeds the shear strength of the particle, resulting in that particle detaching out of its intergranular "pocket" (Dunne, 1990). The mechanics of particle entrainment of noncohesive sediment by seepage was investigated by Howard and McLane (1988). They developed a critical shear stress equation based on the balance of the tractive force due to surface flow, the seepage force, and gravity (Fig. 3). The balance of forces resulted in the following equations:
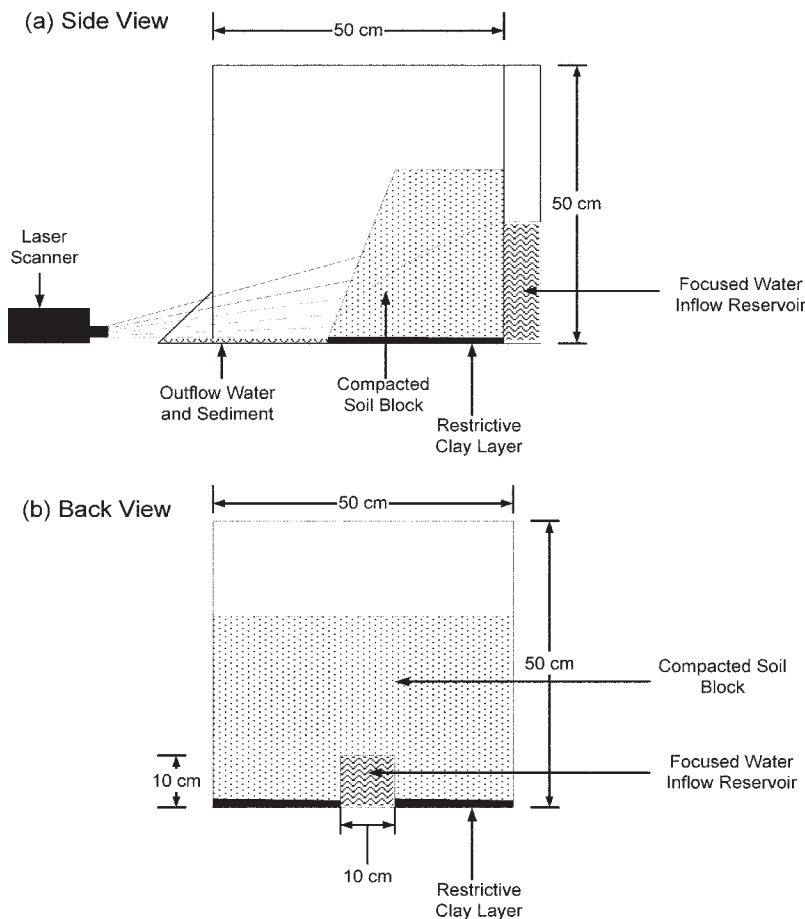

Fig. 4. Three-dimensional laboratory soil block used by Chu-Agor et al. (2008a) to study seepage mechanisms of hillslope instability, including seepage gradient forces and seepage particle mobilization and undercutting.

$$\frac{\tau_c}{(\rho_s-\rho)gd}=C_a\frac{\sin(\beta-\alpha')}{\cos\beta} \qquad [8]$$

$$-C_b\frac{\rho}{\rho_s-\rho}\left[1+\tan\beta\tan(\alpha'+\psi)\right]\sin\alpha'$$

$$C_a=\frac{2C_3}{3C_1} \qquad [9]$$

$$C_b=\frac{12C_2}{nC_1} \qquad [10]$$

where τ_c is the critical shear stress, d is the grain diameter, ψ is the seepage exit angle, β is the angle that the particle makes with another particle, coefficients C_1, C_2, and C_3 are factors that take into account the grain shape and packing effects, and C_a and C_b are constants that can be determined by considering special cases previously analyzed theoretically or experimentally. Note that ψ is the direction of the seepage vector measured clockwise from
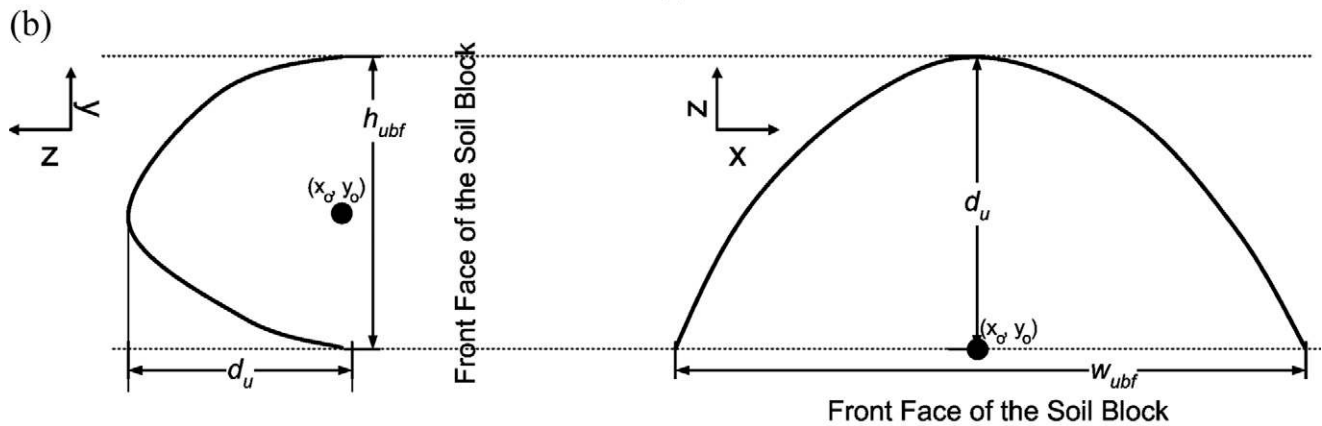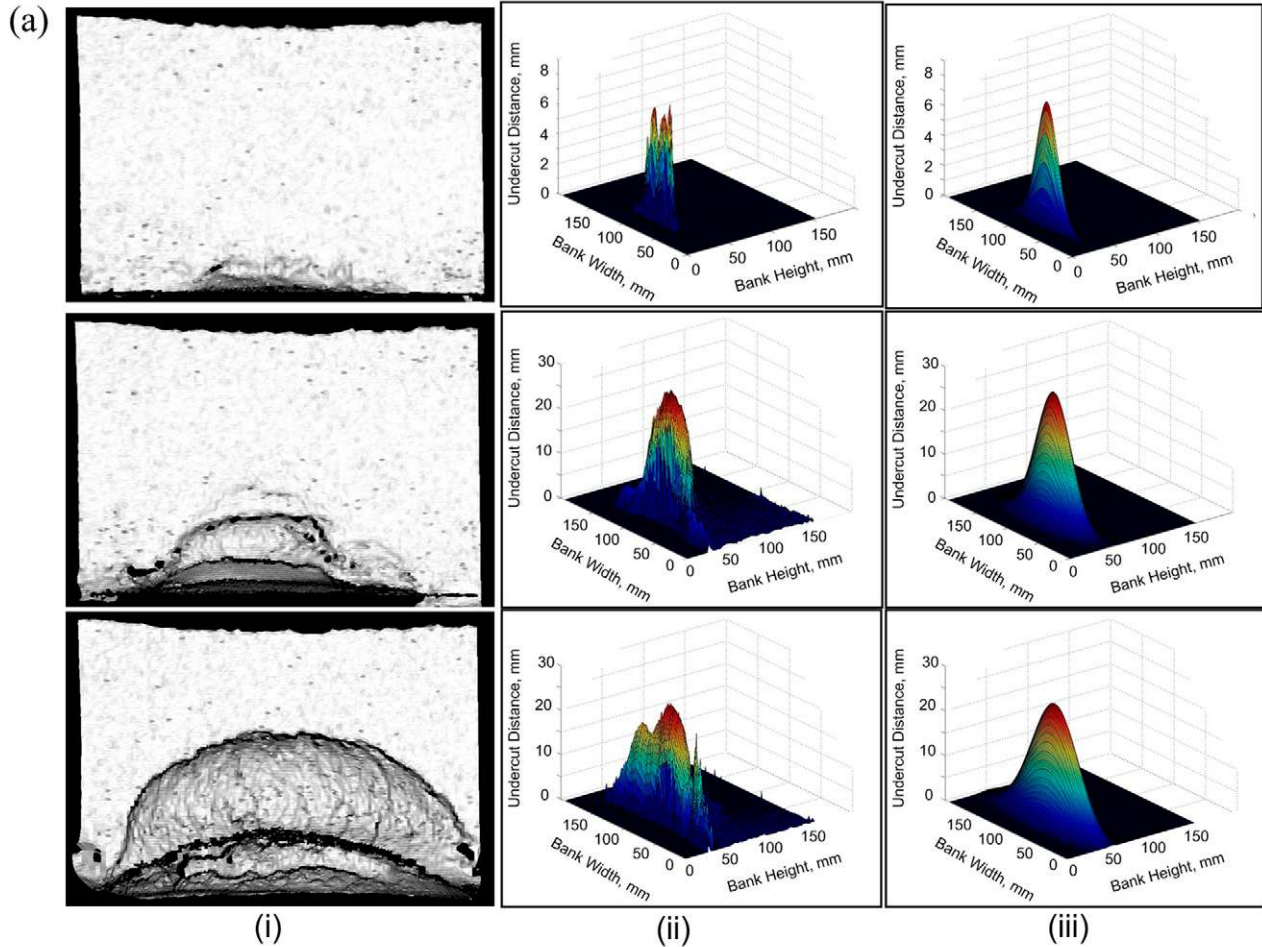

Fig. 5. (a) Bank face view of three-dimensional seepage soil box experiments: (i) time sequence of undercutting; (ii) corresponding data analysis showing the distance of seepage undercutting by particle mobilization on the vertical axis (the face of the bank is the x–y plane); (iii) a five-parameter Gaussian function fit to the seepage particle mobilization data. Data for this figure was taken from Chu-Agor et al. (2008a). (b) Dimensions of the undercut: the maximum undercut distance, $d_u(t)$, the height at the bank face, $h_{ubf}(t)$, and the width at the bank face, $w_{ubf}(t)$. The $h_{ubf}(t)$ and $w_{ubf}(t)$ are functions of the vertical and horizontal spreads (σ_y and σ_x), respectively. From Chu-Agor et al. (2009), with permission from Elsevier.
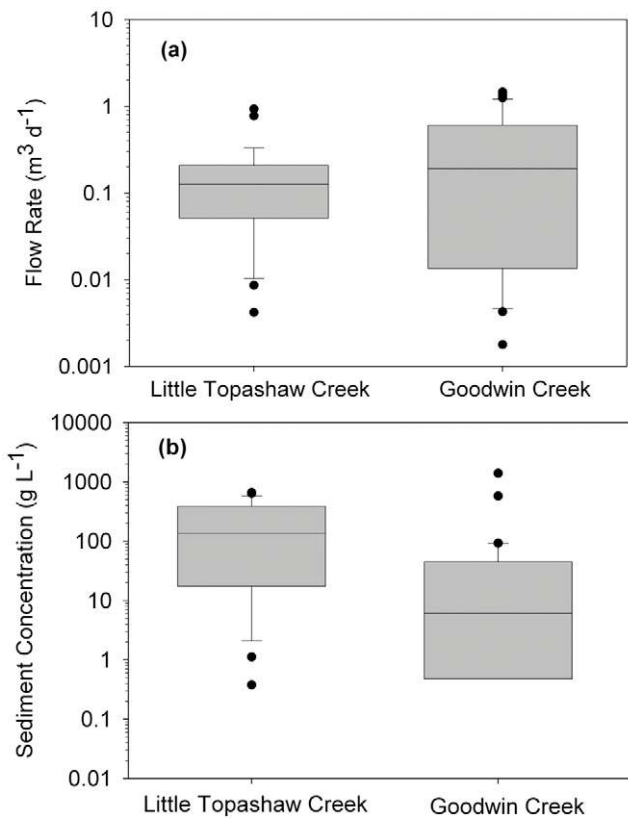
Fig. 6. Box plots of (a) seepage flow rate and (b) seepage sediment concentrations measured at Little Topashaw Creek (Wilson et al., 2007) and Goodwin Creek (Fox et al., 2007) seeps using miniflumes developed by Wilson et al. (2007). Circles represent all data points that lie outside the 10th and 90th percentiles.

the force to the horizontal, while λ is measured clockwise from the inward normal to the bank slope (Fig. 3).

For seepage erosion by particle mobilization, Dunne (1990) adopted the analysis of Howard and McLane (1988) and others wherein the interaction of surface runoff and emergent groundwater was evaluated in terms of the balances of forces acting on a single particle. The movement for a cohesionless particle occurs when

$$i_c > \frac{C_1}{C_2} \frac{(\rho_s - \rho)}{\rho} \frac{\sin(\beta - \alpha')}{\cos(\alpha' + \psi - \beta)} \qquad [11]$$

where i_c is the critical hydraulic gradient.

Lobkovsky et al. (2004) studied the threshold phenomena associated with the onset of erosion using noncohesive glass beads. They derived a critical slope equation with the rationale that slopes greater than the critical were unstable to erosion if there is seepage through them. This critical slope, s_c, relates to the dimensionless critical shear stress (τ_c^*), which was modified to take into account the seepage force:

$$s_c = \frac{\tau_c^* \left[(\rho_s/\rho) - 1 \right]}{a} \qquad [12]$$

where a is the seepage reduction factor, which deals with the fact that grains on the surface experience less seepage force than those several layers deep.
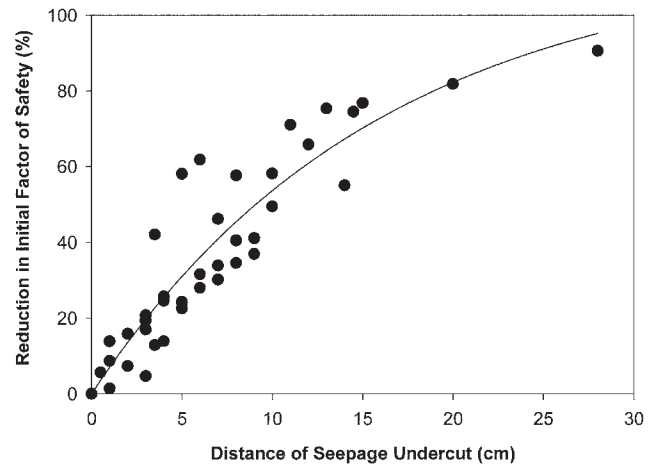

Fig. 7. Reduction in factor of safety relative to the distance of seepage undercutting (Fig. 5) as simulated by Chu-Agor et al. (2008b) for lysimeter experiments mimicking Little Topashaw Creek stream banks in northern Mississippi.

Fewer equations attempt to predict sediment transport by seepage with time (i.e., sediment transport models). Howard and McLane (1988) derived an average long-term sediment transport function for noncohesive soil. They found that in the sapping zone, i.e., the zone of mass wasting by seepage, grains move partly by individual grain motion but mostly by intermittent mass wasting. The amount of seepage-induced mass wasting was assumed to depend on the amount by which the actual slope angle (α') exceeded the critical value (α_c') given by

$$q_{sm} = \exp\left[C_r \left(\frac{\alpha' - \alpha_c'}{\alpha_c'} \right) \right] - 1 \qquad [13]$$

where q_{sm} is the transport rate due to seepage, C_r is a constant, and α_c' is given by the quadratic equation

$$\tan^2 \alpha_c' \left[1 + (C_c + 1) \frac{\tan \psi}{\tan \beta} \right]$$
$$+ \tan \alpha_c' \left[(C_c + 1) \left(\tan \psi + \frac{1}{\tan \beta} \right) \right] - C_c = 0 \qquad [14]$$

where C_c is

$$C_c = \frac{C_a (\rho_s - \rho)}{C_b \rho} \qquad [15]$$

The challenge in using this sediment transport function is estimating the empirical coefficients, C_1, C_2, and C_3 (Eq. [8–11]), which take into account the packing and particle shape effects.

Fox et al. (2006) derived a sediment transport function for seepage erosion of low cohesive stream bank sediment based on two-dimensional lysimeter experiments. Their seepage erosion transport model was based on dimensionless sediment discharge and dimensionless seepage flow stress. Their study showed a power-law relationship between the seepage erosion sediment transport rate (q_{ss}) and seepage rate (q):

$$\frac{q_{ss}}{\sqrt{\left[(\rho_s/\rho) - 1 \right] g d^3}} = a_1 \left[\frac{q}{(s-1) n K_s} \right]^{b_1} \qquad [16]$$

where K_s is the saturated hydraulic conductivity, and a_1 and b_1 are regression parameters specifically derived for loamy sand soils packed within a small range of bulk density. Unlike the transport function of Howard and McLane (1988), this transport model related sediment flux to seepage discharge from the bank. The applicability of the proposed sediment erosion model for utilization under natural field conditions was a concern, however, because the Fox et al. (2006) model was derived using two-dimensional experiments where the width of the bank face was limited, whereas seepage undercutting in the field has a three-dimensional geometry (Fox et al., 2007).

Chu-Agor et al. (2009) developed procedures based on simple geometrical relationships and a seepage erosion sediment transport function for predicting undercut growth and formation as a function of seepage exfiltration velocity. The function was developed with respect to potential data sources in the field, including limited knowledge of the groundwater flow gradient (i.e., measured groundwater table elevation at one observation well or piezometer in the stream bank). Therefore, the equation was derived based on steady-state flow assumptions with average hydraulic gradients, as opposed to the maximum potential seepage gradient in the near-bank domain. Their sediment transport function was represented by an excess-gradient equation, where the gradient, i, was assumed to be based on the steady-state groundwater velocity:

$$E_{rs} = k_{sc}(i - i_c)^a \qquad [17]$$

where E_{rs} is the seepage erosion rate (i.e., a volume of sediment per bank face area per time, $m^3\ m^{-2}\ s^{-1}$), k_{sc} is the seepage erodibility coefficient, i_c is the critical gradient, and a is an exponent reported to be 1.2 for sand and loamy sand soils (Chu-Agor et al., 2009). The steady-state groundwater velocity, v, was estimated from Darcy's law with Dupuit–Forchheimer assumptions:

$$v = \frac{q}{n} = \frac{K_s h \sin(\alpha')}{n L_{sc}} \qquad [18]$$

where q is the flow per area of the seepage undercut per time, L_{sc} is the length of the soil block, K_s is the saturated hydraulic conductivity, and h is the hydraulic head. For cases with undercutting by seepage erosion (Fig. 5), the imposed groundwater gradient, i, was estimated from the steady-state flow based on the imposed hydraulic gradient (i.e., a function of the head, h) and corrected for the depth of undercutting, $d_u(t)$, such that the flow path length is $L_{sc} - d_u(t)$:

$$i = \frac{h \sin(\alpha')}{L_{sc} - d_u(t)} \qquad [19]$$

Increases in $d_u(t)$ increases i by reducing the path length through which the groundwater must discharge.

The critical gradient, i_c, was related to the effective cohesion, c'. Cohesion in soil adds an extra force that has to be exceeded in addition to gravity and water forces before liquefaction can occur. According to Dunne (1990), for soil with some amount of cohesion, an extra force is acting on the soil mass resisting the separation of the mass. Dunne (1990) added that i_c depended on the thickness of the volume that eventually separated. Cohesion therefore is a parameter that can also be used to estimate i_c. Regardless of soil type and packing condition investigated by Chu-Agor et al. (2009), i_c and c' were related through a logarithmic relationship.

Dimensions of the undercut (Fig. 5) were predicted on the basis of a five-parameter Gaussian function (Weisstein, 1999, p. 716–717) for the volume of the eroded surface, where the function was given as

$$z(x,y) =$$
$$d_u(t) \exp\left\{ -\left[\left(\frac{x - x_o}{\sigma_x} \right)^2 + \left(\frac{y - y_o}{\sigma_y} \right)^2 \right] \right\} \qquad [20]$$

where x and y are lateral and vertical directions on the bank face, $z(x,y)$ is the measured seepage undercut distance from the original bank face, x_o and y_o are the center points of the maximum seepage undercut, and σ_x and σ_y are spreads or standard deviations of the seepage undercut. The variables σ_x and σ_y are related to the full width at half-maximum ($FWHM_j$) of the Gaussian function:

$$FWHM_j = 2\sqrt{2\ln(2)}\sigma_j \qquad [21]$$

where j is either x or y (Weisstein, 1999, p. 716–717). Geometric relationships between $d_u(t)$ and σ_x and σ_y were given by Chu-Agor et al. (2009) for their experiments.

From knowledge of $d_u(t)$, σ_x, and σ_y, the five-parameter Gaussian function was simplified to approximate the height (h_u) or width (w_u) of the undercut at different distances along $d_u(t)$. For example, one can solve for the height (h_{ubf}) and width (w_{ubf}) of the seepage undercut at the bank face:

$$h_{ubf} = 2\sigma_y \sqrt{-\ln\left[\frac{\varepsilon}{d_u(t)} \right]}$$
$$w_{ubf} = 2\sigma_x \sqrt{-\ln\left[\frac{\varepsilon}{d_u(t)} \right]} \qquad [22]$$

where ε is a constant close to zero that specifies when a seepage undercut has formed. Similarly, solving for the h_u and w_u at any z, where $z < d_u(t)$, results in the following equations that allow prediction of the entire undercut shape:

$$h_u(z) = 2\sigma_y \sqrt{-\ln\left[\frac{z}{d_u(t)} \right]}$$
$$w_u(z) = 2\sigma_x \sqrt{-\ln\left[\frac{z}{d_u(t)} \right]} \qquad [23]$$

To compute h_{ubf} and w_{ubf} using Eq. [22], it was assumed that ε was equal to the average particle diameter or the median particle

size, d_{50}, of the particle size distribution because an undercut cannot be formed until at least one particle is dislodged from the bank.

With the above sediment transport functions and relationships between $d_u(t)$ and the geometry of the undercut, knowledge of the groundwater velocity exfiltrating from the stream bank can be used to predict the bank geometry resulting from seepage erosion undercutting. First, the effective cohesion (c') of the stream bank seepage layer needs to be input to derive a critical gradient, i_c. Second, the hydraulic gradient, i, needs to be estimated with time. From the measured or modeled hydraulic gradient (i), the erosion rate, $E_{rs}(t)$, can be estimated at each time step, along with the distance of undercut from the previous time step (i.e., an explicit formulation). A negative erosion rate [i.e., $i(t) < i_c$] signifies no transport for that particular time step. For the entire simulated time, the cumulative E_{rs} can be obtained if the layer's bulk density is specified. At a fixed time, the methodology allows the prediction of the volume per unit area of seepage undercut and, correspondingly, $d_u(t)$ through geometrical relationships defined by Chu-Agor et al. (2009). For a two-dimensional bank stability model, only the height of the undercut at the bank face, $h_{ubf}(t)$, is needed, which can be determined using Eq. [22] with σ_y estimated from an empirical power relationship between σ_y and $d_u(t)$. Therefore, the empirical approach used in this research lends itself to being incorporated into a bank stability model with limited information needing to be input by the user.

Constant head

100 to 1200 mm

A. HET Setup Side View

20 mm gravel

Wire mesh

100 mm

Flow measurement

Compacted soil sample

Pinhole

B. Cross-sectional View of Soil Core

Diameter of soil pipe at time t

Preformed pinhole, 6 mm diameter

Fig. 8. Hole erosion test (HET): A. diagram of the setup; B. cross-sectional view of soil core showing enlargement of the initial 6-mm-diameter pinhole to a soil pipe at time t, indicated by the dashed circle.

Soil Piping

It is clear from the literature presented that seepage, whether directly as seepage erosion and sapping or indirectly by the impact of seepage on soil properties, contributes to hillslope and stream bank failure. Piping has been recognized as an important streamflow and erosional process (Gilman and Newson, 1980; Jones, 1981); however, much less work has been done on quantifying internal erosion by pipe flow or incorporating pipe flow processes into hillslope and bank stability analyses. This is in part due to the lack of experimental methods for its assessment. Techniques have been developed, such as the slot erosion test (SET) and the pinhole or hole erosion test (HET), for characterizing the susceptibility to pipe erosion of soil materials used in embankments (Wan and Fell, 2004). Both approaches are based on the excess shear stress equation to describe the sediment flux, q_s (kg s^{-1} m^{-2}), by internal erosion similar to Eq. [17]:

$$q_s = k_{sp}(\tau - \tau_c)^\lambda \qquad [24]$$

where k_{sp} is the erodibility coefficient for internal erosion of a soil pipe and the exponent, λ, is generally taken as unity.

The HET is conducted on a compacted soil core with a 6-mm-diameter hole drilled through the entire length, L, in the core center. Lateral flow is established through the core at a prescribed head, 50 to 1200 mm at the upstream and 100 mm at the downstream ends, to produce a constant hydraulic gradient ($\Delta h/L$) (Fig. 8). The internal erosion of the pipe, i.e., the rate of pipe enlargement, cannot be measured with this setup, therefore the flow rate, Q_t, is used to calculate the pipe diameter, D_t, at time t by

$$\text{Laminar flow:} D_t = \left(\frac{16 Q_t F_{Lt}}{\pi \rho g \Delta h/L} \right)^{1/3} \qquad [25]$$

$$\text{Turbulent flow:} D_t = \left(\frac{16 Q_t^2 F_{Tt}}{\pi^2 \rho g \Delta h/L} \right)^{1/5} \qquad [26]$$

where the appropriate friction factor, F_{Lt} or F_{Tt} is used. The sediment flux is thus

$$q_s = \frac{\rho}{2} \frac{\Delta D_t}{\Delta t} \qquad [27]$$

and the shear stress at time t, τ_t, is

$$\tau_t = \rho_w g \frac{\Delta h}{L} \frac{D_t}{4} \qquad [28]$$

where ΔD_t is the change in the soil pipe diameter.

The SET is performed by compacting a soil bed in a Plexiglas box in which a 2.2-mm-wide by 10-mm-deep by 1000-mm-long slot is formed at the center depth line of the soil bed along the outside edge such that it is visible from the Plexiglas side (Fig. 9). An upstream and downstream prescribed head is established on the slot as with the HET; however, the internal
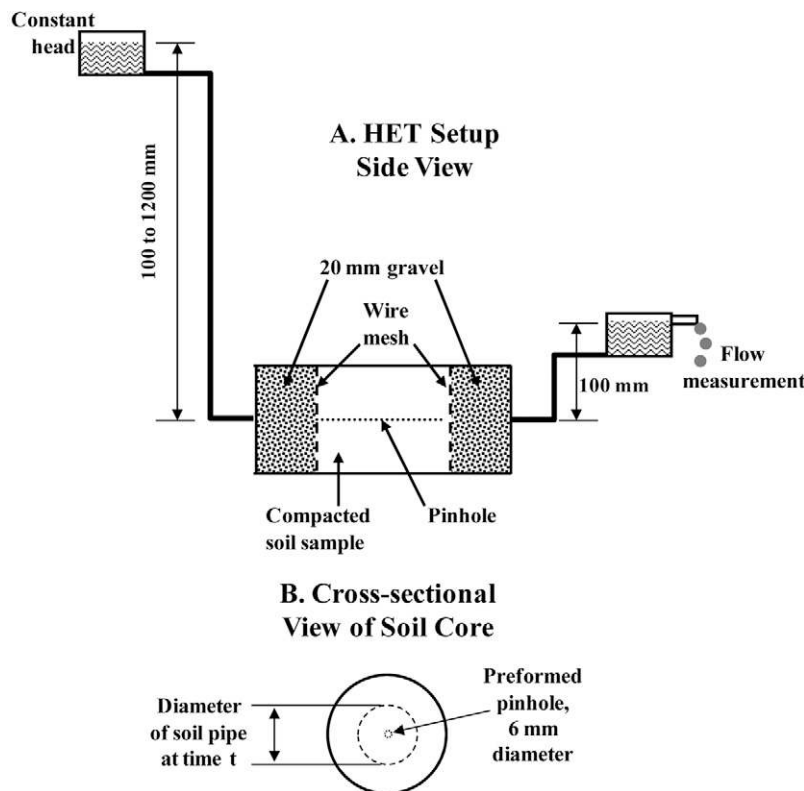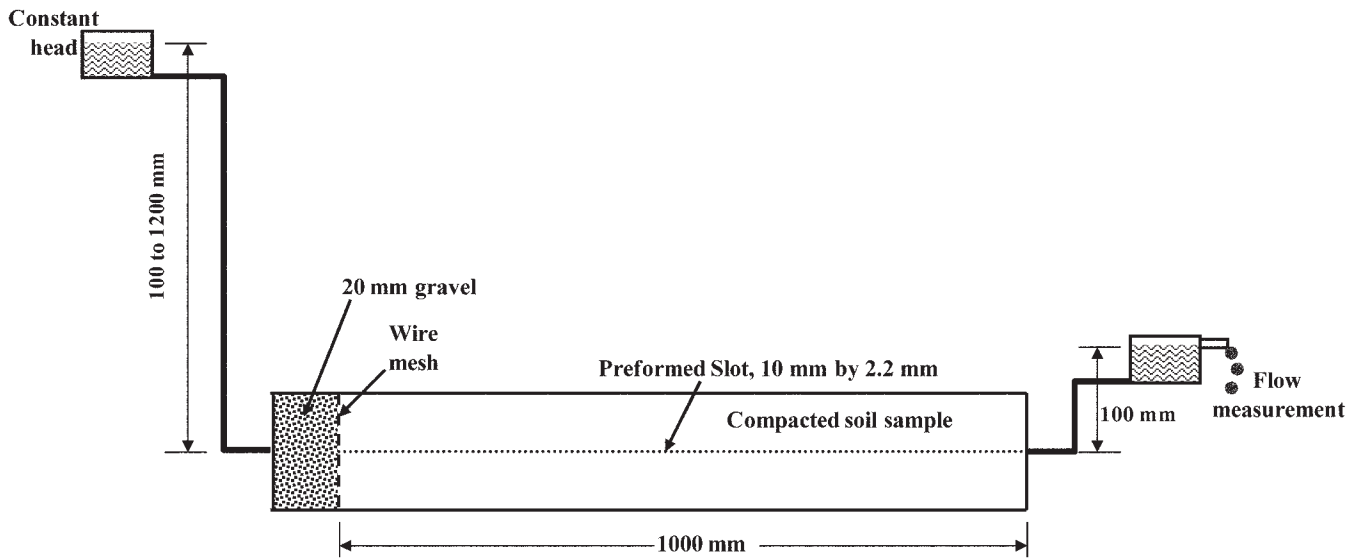
Fig. 9. Diagram of the slot erosion test (SET) setup. The slot is formed at the center depth line of the soil bed along the edge of the Plexiglas box. Sediment concentration and flow rate are measured from the slot.

erosion of the slot is monitored by digital imaging (Fig. 10). With the SET, the mass of soil loss with time, M_t, is directly measured and the cross-sectional area, A_t, of the slot is calculated from direct measurements of the slot diameter, D_t.

Thus, the sediment flux can be calculated by

$$q_s = \frac{1}{A_w}\frac{\Delta M_t}{\Delta t} = \frac{\rho_w}{C_w}\frac{\Delta A_t}{\Delta t} \qquad [29]$$

where A_w is the wetted area, which equals the product of the wetted circumference around the pipe, C_w, at time t and the pipe length, L. For both methods, the sediment flux is plotted against the shear stress calculated by Eq. [28]. Linear regression, i.e., Eq. [24], provides an estimate of the critical shear stress (intercept) and soil-pipe erodibility coefficient (slope).

Wilson (2009) used a modification of these methods to describe pipe erosion for a 1-cm soil pipe in a loess soil, immediately above (1 cm) an impermeable layer, in the center of a soil bed under conditions of steady-state flow into the soil pipe (Supplemental Video 3: Continuous steady-state pipe flow experiment; Supplemental Video 4: Discontinuous soil pipe flow experiment). The experiments were designed to address tunnel collapse related to ephemeral gully erosion; however, by nature of the soil pipe exiting the soil bed face, they provided insight into the role of pipe erosion on bank failure. The initial

10-mm-diameter soil pipe enlarged to >50 mm due to internal erosion, but tunnel collapse was not observed.

When pipe flow was combined with sheet flow due to rainfall on the soil surface, the combination consistently resulted in mass wasting of the bank face around the pipe and the soil loss by mass wasting was not significantly different from that by internal erosion of the pipe. While flow into the continuous soil pipe was constant, flow through the soil pipe was highly dynamic due to internal erosion clogging the pipe until minor pressure buildups forced out the debris plug. As a result of the rapid flow through
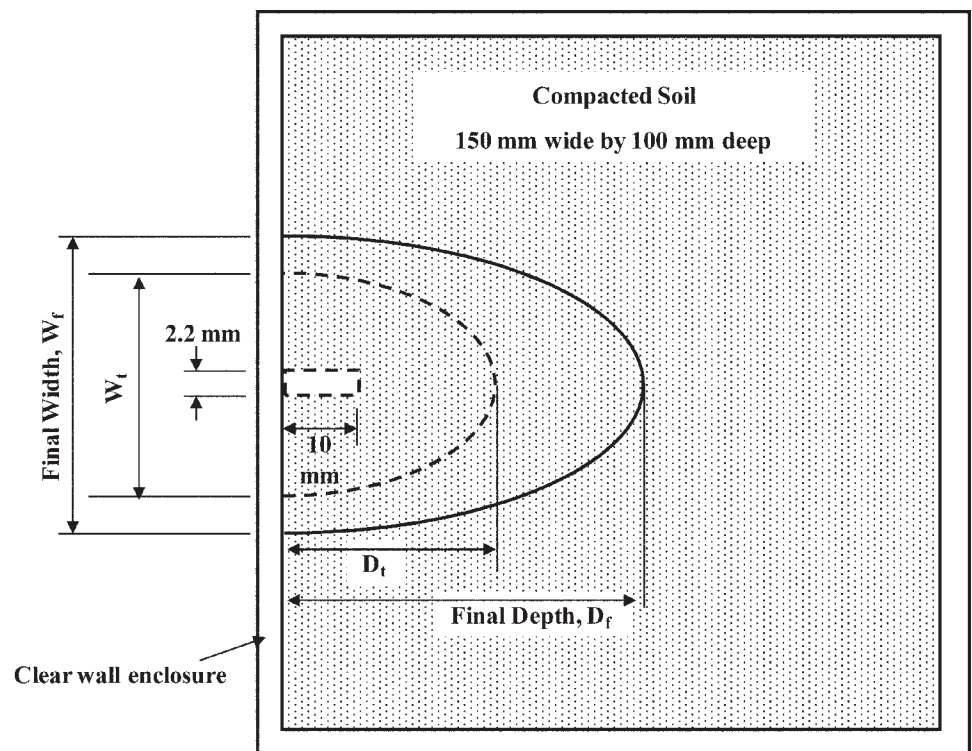

Fig. 10. Cross-sectional view of slot erosion test soil bed with an initial slot, 2.2 mm wide by 10 mm deep, along the clear outside wall. The enlargement of the pipe width and depth into the soil bed at time t (W_t and D_t, respectively) is recorded. The final width, W_f, and final depth, D_f, of the slot is measured at the end of test.

the soil pipe, hydraulic nonequilibrium between the pipe and soil matrix resulted in hydraulic gradients, as observed by tensiometers in the soil adjacent to the soil pipe, through the soil bed in the opposite direction of flow through the soil pipe. Such behavior was reported on forested hillslopes by De Vries and Chow (1978) and was observed by Simon and Wells (2006) at a stream bank seep that was prone to failure.

Kosugi et al. (2004) conducted experiments on soil pipes in beds in which three parallel perforated pipes (10-mm o.d.), spaced 1.8 cm apart, were centered immediately (1 cm) above the impermeable bottom. Soil pipes were either open at the lower outlet with a simulated stream stage of 3-cm depth, or discontinuous by ending 15 cm upslope from the face. The upper ends of these soil pipes were not connected to the water reservoir at the upper face but were embedded with their opening 25 cm downslope. The soil pipes open at the outlet served to reduce pore water pressures, i.e., a drainage pipe, of the soil bed, thereby increasing hillslope stability. This is consistent with the speculations by Sidle et al. (2006) that vegetation can provide old root channels that facilitate preferential drainage of hillslopes, thereby increasing their stability. Once the open pipes clogged, however, pore water pressures built up. The discontinuous soil pipes of Kosugi et al. (2004) caused an increase in pore water pressures at the lower end, which they proposed could cause hillslope failure.

Such experiments provide new insights into the soil piping processes and help to explain field observations on hillslopes and stream banks that were previously mere speculation or what Sidle et al. (2006) called "unproven scenarios for pore water pressure accretion and landslide initiation."

LIMITATIONS AND KNOWLEDGE GAPS
Characterizing Soil Properties of Seepage Layers

One of the main difficulties in predicting hillslope and stream bank instability is the lack of soil property data and the need for improved methods of measuring the pertinent properties. Subsurface flow contributions are typically associated with duplex soils, i.e., a water-restricting layer, which may involve thin (10-cm) layers with subtle (less than one order of magnitude) contrasts in hydraulic conductivity. Thus, detailed site characterization of soil properties is crucial for a priori predictions. This may require development of surrogate or nonintrusive measures for characterizing the properties of soil layers in extreme environments, e.g., unstable stream banks and steep terrains, and improvements in pedotransfer functions for predicting hydraulic properties.

While some of the soil properties presently used for stability analysis, such as the densities of the fluid, sediment, and bulk soil, are readily available, other properties and coefficients are not available and methods for their in situ characterization often do not exist. Even the primary erosion properties (e.g., shear strength, effective cohesion, erodibility, and critical shear stress) are not easily measured nor are they well understood with regard to their codependence on other soil properties.

For instance, cohesion is arguably one of the most important parameters used in stability analysis. The bonding of particles by cohesive forces is affected by air–water–particle surface tensions, intermolecular interactions, chemical cementation reactions, and microbial bonding actions. Despite its significance, soil cohesion values are not readily available. Instead, there are indirect measurements such as moduli of rupture (Kemper and Rosenau, 1984), tensile strength (Munkholm and Kay, 2002; Blanco-Canqui et. al., 2005), and aggregate stability (Nimmo and Perkins, 2002). Thoman and Niezgoda (2008) listed the following as the most important properties controlling erosion: clay content, plasticity index, mean particle size, organic matter content, water content, and Na adsorption ratio. While these properties affect soil cohesion, none of these properties are directly included in hillslope and bank stability analyses. Given that the aggregate stability of cohesive stream bank materials depend on the physical–chemical properties of the clay minerals (Reichert et al., 2009), chemical interactions between the exfiltrating groundwater and the stream bank materials are potentially occurring, which can affect their resistance to erosion. It has been commonly observed that subsurface flow through forested hillslopes and into stream channels at the initiation of storm flow, i.e., the initial rise of a hydrograph, is dominated by new water (Wilson et al., 1991a). Thus, this water has a low ionic strength, which can enhance sediment detachment in soil pipes (Wilson et al., 1991b). This could explain why turbidity and sediment concentrations are high at the initiation of runoff (Dabney et al., 2006). The effect of subsurface flow chemistry on cohesion properties of hillslopes and stream banks or on the soil erodibility parameters has not been studied. There is a need for pore-scale research to better understand and predict such phenomena.

Development of Improved Erosion Equations for Seepage and Piping

The most universally accepted erosion prediction equation is the excess shear stress equation:

$$D_c = k_c \left(\tau - \tau_c \right)^b \qquad [30]$$

where D_c is the flow detachment capacity, k_c is the concentrated flow soil erodibility, τ and τ_c were defined above, and b is an exponent. The relationship between D_c and $\tau - \tau_c$ is typically assumed to be linear, $b = 1$. A fairly extensive database exists for k_c and τ_c (Knapen et al., 2007) for surface soils experiencing concentrated surface flow. It is not clear how these values relate to the substantially less available soil erodibility parameters k_{se} (Eq. [17]) and k_{sp} (Eq. [24]) for seepage and soil piping, respectively, or their associated shear stress values in Eq. [8] and [24].

It is clear from the analogous surface flow parameters that there is a great deal of variability in these values that is caused by differences in methods and their application. For this reason, Knapen et al. (2007) did not include values from the impinging submerged jet test in their review even though this is a standardized method (ASTM International, 2007) developed for in situ measurement of k_c and τ_c (Hanson and Cook, 1997).

Even by restricting the database to the linearized values based on concentrated flow experiments in laboratory flumes

and field plots, it is clear that these soil erosion resistance properties are not time-invariant, intrinsic soil properties. These parameters change with time as soil and environmental characteristics change, such as by soil management or hydrologic conditions. Knapen et al. (2007) found that tillage affected soil erodibility, k_c, but not critical shear stress. Owoputi and Stolte (2001) found that seepage affects the rate of erosion by impacting the erodibility. Huang and Laflen (1996) and Gabbard et al. (1998) found that the erosion rate significantly increased due to seepage exfiltration, which Howard and McLane (1988) proposed was due to the reduction of effective shear stress.

Thoman and Niezgoda (2008) noted that many soil properties can affect soil erodibility and critical shear stress. They determined k_c and τ_c of channels using the in situ jet device and developed correlations between critical shear stress and soil cohesion properties. The in situ jet test was developed for submerged, i.e., streambed, conditions and it is not clear how well it represents the soil erosion properties of unsaturated soil profiles; this is an area needing further work. Regardless of the device used, similar correlations need to be developed for conditions of seepage and pipe flow erosion for soil erodibility (k_{se} and k_{sp}) and critical shear for subsoils.

Another difficulty in predicting hillslope and stream bank instability is the interaction of the various mechanisms among themselves as well as with other processes. For example, if the seepage velocity does not exceed a critical threshold, particles will not be transported out of the bank, i.e., no seepage erosion. Seepage gradients still exert physical forces on stream bank sediment, however, and soil properties representing resistance to erosion by other mechanisms may be altered. Determining under what conditions any one of these processes becomes the controlling mechanism or how they interact synergistically has yet to be determined.

The interaction of soil pipes on hillslope hydrology is complicated due to their potential to provide drainage of the hillslope (Sidle et al., 2006), thereby increasing the slope stability by increased shear strength. High flow velocities inside soil pipes result in internal erosion, however, and if the sediment transport capacity of the soil pipe is exceeded, then clogging of the soil can suddenly cause pressure buildups, resulting in slope failure. The interactions of these mechanisms have not been fully explored.

Better methods need to be developed for describing internal erosion related to soil piping, and experiments need to be conducted under many more conditions in which pipe flow contributes to hillslope and stream bank failure. For instance, what size macropore is necessary to initiate internal erosion, thereby producing a soil pipe? Given that seepage may occur with perched heads of <5 cm, do macropores need to be immediately above the water-restrictive layer to be hydrologically active? What size soil pipe is necessary for internal erosion to result in clogging and, therefore, pressure buildups, and is this phenomenon related to the aggregate size distribution and soil texture, i.e., particles or aggregates of sufficient size to clog the pore when dislodged? Additionally, numerical techniques need to be developed for modeling soil piping processes. One approach that has provided

insights into the pipe flow process has been to apply a Richards' equation approach to the flow using a high K_s value to represent the soil pipe (Nieber and Warner, 1991; Kosugi et al., 2004). Unlike the case of stream bank stability, in which variably saturated flow codes based on the solution of Richards' equation have been integrated with geotechnical models of bank stability, e.g., GEOSLOPE codes (Chu-Agor et al., 2008b), numerical models have not been developed for integrating soil pipe flow into hillslope stability. The continuum approach of solving Richards' equation for variably saturated flow is limited to laminar flow, which is not applicable to pipe flow conditions, and water retention properties are problematic because soil pipes are either water filled or empty. Additionally, a Richards' equation approach in which the soil pipe is represented by a boundary within the flow domain suffers from the fact that the flow domain changes with time as the soil pipe enlarges by internal erosion, and it is not clear what boundary condition to apply to such a soil pipe, particularly given that as the soil pipe enlarges or flow diminishes, the soil pipe may be partially filled.

Influence of Vegetation on Seepage Processes

The interaction between subsurface flow mechanisms and vegetation becomes an interesting facet requiring future research efforts. The cohesion of bulk soil is affected by the tensile strengths of roots and fungal hyphae that intertwine among the bonded particles. Plant roots have high tensile strength but weak compressive strength, whereas soil has high compressive strength but low tensile strength, so that they form a strong composite material (Pollen, 2007). The impact of roots on soil strength can be represented by adding an apparent root cohesion term, c_r, in Eq. [1] (Abernethy and Rutherfurd, 2001). Vegetation effects on cohesive properties of stream banks are commonly assessed either as an increased shear strength resistance to failure by root-permeated soil (Wu et al., 1988) or relationships between root and soil properties developed from direct measurements on roots (Pollen and Simon, 2005; Pollen, 2007). Abernethy and Rutherfurd (2001) measured the tensile strength of individual debarked roots in the laboratory. In the field, however, roots have the added effect of the attractive forces between the root fibers and the soil matrix. Abernethy and Rutherfurd (2001) developed a field method for measuring the load required to pull a root out of a bank face. Pollen and Simon (2005) reported values of root tensile strength for a variety of species using the root-puller method. From these measurements, they developed a fiber bundle model, RipRoot, for use with bank stability assessment. The fiber bundle model allows for progressive breaking of roots, as opposed to simultaneous breaking of all roots, with a redistribution of the stress to the remaining roots. Mickovski et al. (2009) also measured the tensile strength of individual roots in the laboratory but used these measures in conjunction with measures of shear test on bulk soil with roots compared with fallow bulk soil. They found that the progressive failure fiber bundle model of Pollen and Simon (2005) gave better results than catastrophic failure models, which overpredicted soil–root

reinforcement by 33%. The assessment of root impacts on soil strength is a fairly new field of science that needs significantly greater work. Measurements for different plant species and their relationships to soil properties, e.g., soil type, clay content and mineralogy, organic matter, and water content and pressure, need to be established.

Simon and Collison (2002), Pollen and Simon (2005), and Pollen (2007) have indicated that vegetation can have both advantageous and disadvantageous effects on stability. One of the advantageous effects is the removal of soil water from the root zone, contributing to the persistence of negative pore-water pressures in the stream bank. Sidle et al. (2006) stated that forests protect hillslopes from landslides by (i) increased evapotranspiration and thus drying of the hillslope, (ii) increased cohesion of the soil matrix by roots thus increasing the soil shear strength, and (iii) providing macropores (secondary permeability) for hillslope drainage. Of these, they stated that the effect of roots on the soil shear strength was the most important. Disadvantageous effects of vegetation include the increased load on the bank and the potential for preferential flow, along with clogging from internal erosion, along old root channels. More work is needed beyond the few studies performed to date, especially on the relationship between vegetation and subsurface flow.

Cancienne et al. (2008) noted that stream bank instability by seepage erosion undercutting was as important as stability mechanisms such as riparian vegetation. Cancienne and Fox (2008) performed some preliminary three-dimensional soil block experiments in the laboratory with transplanted switchgrass (*Panicum virgatum* L.) grown for approximately 2 mo. Their findings indicated that the presence of visible roots on the bank surface controlled the lateral extension of the seepage headcut. Increases in root cohesion, as quantified through the root area/soil ratio and the tensile strength of the roots, increased the required time to failure when exposed only to groundwater instability forces. Future research is necessary to determine if recent advances in crop growth modeling can also play a role in linking and relating these instability and stability mechanisms.

Scaling Seepage Processes to Watershed Scale

At larger spatial scales, linking of groundwater flow, fluvial hydraulics, and stream bank stability models suggests the need to scale up to the watershed level. The concept used in many watershed models, that runoff generation from a field occurs at a particular location in the landscape, meshes with the commonly observed occurrence of seepage exfiltration at specific hillslope locations and points along stream banks. Measurements of seepage flow rates and sediment discharges at a point in time for specific hillslope or stream bank locations does not take into account the effect of sediment transport on the convergence of upslope groundwater pathways. Hagerty (1991) suggested that the formation of cavities on the bank face accelerates groundwater flow to that location. Scaling up from stream bank transects or reaches with seepage erosion to the watershed scale will require hydrologic simulation models at the watershed scale that can simulate heterogeneous subsurface flow scenarios. Existing watershed-scale models are significantly lacking in their ability to predict such heterogeneities in flow paths and do not consider changes in time in these flow paths due to erosion dynamics. The concepts of dynamically changing discrete source areas for runoff need to be included in future research efforts to determine if such concepts can predict the occurrence of hillslope and bank failures by subsurface flow.

SUMMARY AND CONCLUSIONS

We have reviewed the roles of subsurface flow on the geotechnical properties of hillslopes and stream banks that can lead to failure. The roles of seepage, e.g., seepage gradients, seepage erosion, and sapping, along with preferential flow through discrete soil pipes, on the stability of hillslopes and stream banks were discussed and mathematical relationships describing these processes were presented. Generally speaking, existing geotechnical models that utilize a spatially and temporally invariant hydrostatic vertical pressure distribution are underestimating the effects of these subsurface flow mechanisms of instability.

According to Crosta and di Prisco (1999), to understand the onset of stream bank instability, it is important to point out that collapse is the final result of a complex chain of events taking place during a certain time period. The analysis is complex because of the partial saturation of the materials, the three-dimensional geometry of the problem, the heterogeneity of the materials, and because the individual physical, geotechnical, and hydraulic forces acting on the soil mass cannot be separated. Thus, stream bank and hillslope instability by groundwater mechanisms remains a field requiring significantly greater research (Committee on Hydrologic Science, National Research Council, 2004). Progress will require work at both the pore scale, in terms of understanding the dynamics of soil-water and soil-chemical interactions with soil physical properties, and plant-root relations with soil strength, and at a hillslope and stream bank scale in integrating the geotechnical, soil physics, and hydrologic mechanisms, and their linkages to watershed-scale response. This will require a multidisciplinary approach that should include significant involvement of soil physicists and engineers.

Future research efforts should target:

· Sensitivity analysis on subsurface flow and hillslope or bank stability to determine the most critical soil and hydrologic parameters controlling seepage outflow predictions and slope stability.

· Development of improved methods for characterizing soil properties related to hillslope and stream bank stability or development of correlations with surrogate soil properties.

· Determination of the effects of solution chemistry, vegetation, and soil management and land use effects on the controlling erosion and stability parameters.

· Laboratory and field-scale experiments on pipe-flow erosion mechanisms of hillslope and bank instability, determining relationships among flow rates, perched

water table heads, pore diameters, and soil properties that result in instability.

· Controlled field experiments, similar to the three-dimensional, laboratory-scale seepage erosion and sapping experiments, for conditions with natural heterogeneity and anisotropy.

· Laboratory studies in which seepage erosion forces are combined with streamflow hydraulic forces, which, combined with numerical modeling of multiple simultaneous forces, will determine the prevalence of different seepage and streamflow mechanisms of bank failure.

· Further derivation, refinement, and development of seepage erosion undercutting relationships, including a database of parameters for an excess gradient equation or similar empirical relationships for multiple soil types and packing conditions.

· Improved models for describing internal erosion by soil-pipe flow and integration of such models into hillslope and stream bank scale stability models.

· Numerical modeling studies to evaluate the necessary conditions for perched seepage to occur, highlighting when this mechanism needs to be considered in bank stability analyses, and inclusion of the potential for seepage erosion in geomorphic assessments of streams, such as water-restrictive layers and undercut banks.

APPENDIX

a	reduction factor used in Lobkovsky et al. (2004) to account for less seepage force experienced by soil grains on the hillslope surface
a_1, b_1	empirical regression parameters of the Fox et al. (2006) sediment transport equation
A_t	cross-sectional area of the slot in the slot erosion test, m^2
b	dimensions of the failed soil block in the Chu-Agor et al. (2008a) equation, m
c	apparent cohesion, kPa
c'	effective cohesion, kPa
C_1, C_2, C_3	empirical coefficient in the Howard and McLane (1988) equation for grain shape and packing effects
C_a, C_b, C_c	empirical coefficients in the Howard and McLane (1988) equation
C_r	constant in the Howard and McLane (1988) sediment transport rate equation
C_w	wetted circumference around a soil pipe, m
d	grain diameter, m
d_{50}	mean particle size diameter, m
d_u	depth of seepage undercutting in the Chu-Agor et al. (2009) equation, m
D	soil depth to bedrock in the Iida (2004) relationship, m
D_t	soil pipe or soil slot diameter, m
e	void ratio
E_{rs}	seepage erosion sediment transport rate in the Chu-Agor et al. (2009) equation, m^3 m^{-2} s^{-1})
F_{Lt}, F_{Tt}	friction factor for flow through a soil pipe under laminar and turbulent flow, respectively
g	gravitational acceleration, m s^{-2}
G	specific gravity
h	hydraulic head, m
h_u	height (vertical dimension) of the seepage undercut, m
h_{ubf}	height (vertical dimension) of the seepage undercut at the bank face, m
H_{cr}	critical depth of saturated soil for hillslope failure in the Iida (2004) equation, m
i	seepage gradient

i_c	critical hydraulic gradient for particle mobilization by seepage
k_{se}	seepage erodibility coefficient in the Chu-Agor et al. (2009) sediment transport equation, m^3 m^{-2} s^{-1}
k_{sp}	erodibility coefficient for the internal erosion of a soil pipe, s m^{-1}
K_s	saturated hydraulic conductivity, m s^{-1}
L	length of the soil column, m
L_{sc}	length of the soil across which the gradient is measured in the Chu-Agor et al. (2009) sediment transport equation, m
M_t	mass of soil erosion by a soil pipe, kg
n	soil porosity
q	Darcy groundwater velocity, m s^{-1}
q_s	sediment flux by internal erosion of a soil pipe, kg m^{-2} s^{-1}
q_{ss}	sediment transport rate in the Fox et al. (2006) equation, m^2 s^{-1}
q_{sm}	dimensionless sediment transport rate due to seepage (Howard and McLane, 1988)
Q_t	flow rate through a soil pipe, m^3 s^{-1}
s	soil shear strength, kPa
s_c	critical slope for particle mobilization by seepage
u_a	pore air pressure, kPa
u_w	pore water pressure, kPa
v	steady-state groundwater velocity (m/s)
w_u	width (lateral dimension) of the seepage undercut, m
w_{ubf}	width (lateral dimension) of the seepage undercut at the bank face, m
x, y	distances, m
x_o, y_o	center points of the maximum seepage undercut distance, m
$z(x,y)$	seepage undercut distance from the original bank face in the Chu-Agor et al. (2009) sediment transport equation, m
Δz	depth from the surface to where mobilization by sapping occurs in the Dunne (1990) equation, m
α'	bank angle, $^\circ$
α_c'	parameter of the Howard and McLane (1988) sediment transport equation, $^\circ$
β	angle that a soil particle makes with another particle, $^\circ$
γ_{sat}	saturated unit weight of the soil, N m^{-3}
γ_{uns}	unsaturated unit weight of the soil, N m^{-3}
γ_w	unit weight of water, N m^{-3}
ε	constant that specifies when a seepage undercut has formed (m)
λ	seepage vector angle measured clockwise from the inward normal to the bank slope, $^\circ$
ρ	fluid density, kg m^{-3}
ρ_b	soil bulk density, kg m^{-3}
ρ_s	sediment density, kg m^{-3}
σ_n	total normal stress, kPa
σ_x, σ_y	spreads (standard deviations) of the seepage undercut, m
τ_c	critical shear stress, kPa
ϕ^b	rate of increase in soil strength with increasing matrix suction, $^\circ$
ϕ'	angle of internal friction, $^\circ$
ψ	seepage exit angle in the Howard and McLane (1988) equation measured clockwise from the seepage force to the horizontal, $^\circ$

REFERENCES

Abernethy, B., and I.D. Rutherfurd. 2001. The distribution and strength of riparian tree roots in relation to riverbank reinforcement. Hydrol. Processes 15:63–79.

ASTM International. 2007. D5852-00: Standard test method for erodibility determination of soil in the field or in the laboratory by the jet index method. *In* Book of standards. Vol. 0408. ASTM International, West Conshohocken, PA.

Blanco-Canqui, H., R. Lal, L.B. Owens, W.M. Post, and R.C. Izaurralde. 2005. Mechanical properties and organic carbon of soil aggregates in the northern Appalachians. Soil Sci. Soc. Am. J. 69:1472–1481.

Bocco, G. 1991. Gully erosion, processes, and models. Prog. Phys. Geogr. 15:392–406.

Bryan, R.B., and J.A.A. Jones. 1997. The significance of soil piping processes: Inventory and prospect. Geomorphology 20:209–218.

Budhu, M., and R. Gobin. 1996. Slope stability from ground-water seepage. J. Hydraul. Eng. 122:415–417.

Cancienne, R., and G.A. Fox. 2008. Laboratory experiments on three-dimensional seepage erosion undercutting of vegetated banks. Pap. 084107. Am. Soc. Agric. Biol. Eng., St. Joseph, MI.

Cancienne, R., G.A. Fox, and A. Simon. 2008. Influence of seepage undercutting on the root reinforcement of streambanks. Earth Surf. Processes Landforms 33:1769–1787.

Chu-Agor, M.L., G.A. Fox, R. Cancienne, and G.V. Wilson. 2008a. Seepage caused tension failures and erosion undercutting of hillslopes. J. Hydrol. 359:247–259.

Chu-Agor, M.L., G.A. Fox, and G.V. Wilson. 2009. A seepage erosion sediment transport function and geometric headcut relationships for predicting seepage erosion undercutting. J. Hydrol. 377:155–164.

Chu-Agor, M.L., G.V. Wilson, and G.A. Fox. 2008b. Numerical modeling of bank stability by seepage erosion. J. Hydrol. Eng. 13:1133–1145.

Committee on Hydrologic Science, National Research Council. 2004. Groundwater fluxes across interfaces. Natl. Acad. Press, Washington, DC.

Crosta, G., and C. di Prisco. 1999. On slope instability induced by seepage erosion. Can. J. Geotech. 36:1056–1073.

Dabney, S.M., M.A. Locke, and R.W. Steinriede. 2006. Turbidity sensors track sediment concentration in runoff from agricultural fields. p. 345–352. *In* Proc. Federal Interagency Sediment. Conf., 8th, Reno, NV. 2–6 April 2006. U.S. Gov. Print. Office, Washington, DC.

Darby, S.E., M. Rinaldi, and S. Dapporto. 2007. Coupled simulations of fluvial erosion and mass wasting for cohesive river banks. J. Geophys. Res. 112:F03022, doi:10.1029/2006JF000722.

De Vries, J., and T.L. Chow. 1978. Hydrologic behavior of a forested mountain soil in Coastal British Columbia. Water Resour. Res. 14:935–942.

Dunne, T. 1990. Hydrology, mechanics, and geomorphic implications of erosion by subsurface flow. p. 11–28. *In* C.G. Higgins and D.R. Coates (ed.) Groundwater geomorphology: The role of subsurface water in earth-surface processes and landforms. Spec. Pap. 252. Geol. Soc. Am., Denver, CO.

Faulkner, H. 2006. Piping hazard on collapsible and dispersive soils in Europe. p. 537–562. *In* J. Boardman and J. Poesen (ed.) Soil erosion in Europe. John Wiley & Sons, Chichester, UK.

Foster, M.A., R. Fell, R. Davidson, and C.F. Wan. 2002. Estimation of the probability of failure of embankment dams by internal erosion and piping using event tree methods. ANCOLD Bull. 121. Aust. Natl. Comm. on Large Dams, Melbourne, VIC.

Foster, M.A., R. Fell, and M. Spannangle. 2000. The statistics of embankment dam failures and accidents. Can. Geotech. J. 37:1000–1024.

Fox, G.A., G.V. Wilson, R.K. Periketi, and R.F. Cullum. 2006. Sediment transport model for seepage erosion of stream bank sediment. J. Hydrol. Eng. 11:603–611.

Fox, G.A., G.V. Wilson, A. Simon, E. Langendoen, O. Akay, and J.W. Fuchs. 2007. Measuring streambank erosion due to ground water seepage: Correlation to bank pore water pressure, precipitation, and stream stage. Earth Surf. Processes Landforms 32:1558–1573.

Fredlund, D.G., and H. Rahardjo. 1993. Soil mechanics for unsaturated soils. John Wiley & Sons, New York.

Fredlund, D.G., and S.K. Vanapalli. 2002. Shear strength of unsaturated soils. p. 329–361. *In* J.H. Dane and G.C. Topp (ed.) Methods of soil analysis. Part 4. SSSA Book Ser. 5. SSSA, Madison WI.

Gabbard, D.S., C. Huang, L.D. Norton, and G.C. Steinhardt. 1998. Landscape position, subsurface hydraulic gradients and erosion processes. Earth Surf. Processes Landforms 23:83–93.

Gerke, H.H. 2006. Preferential flow descriptions for structured soils. J. Plant Nutr. Soil Sci. 169:382–400.

Ghiassian, H., and S. Ghareh. 2008. Stability of sandy slopes under seepage conditions. Landslides 5:397–406.

Gilman, K., and M.D. Newson. 1980. Soil pipes and pipeflow: A hydrological study in upland Wales. Brit. Geomorphol. Res. Group Res. Monogr. Ser. 1. Geobooks, Norwich, UK.

Gomi, T., R.C. Sidle, and D.N. Swanston. 2004. Hydrogeomorphic linkages of sediment transport in headwater streams, Maybeso Experimental Forest, southeast Alaska. Hydrol. Processes 18:667–683.

Hagerty, D.J. 1991. Piping/sapping erosion: 1. Basic considerations. J. Hydraul. Eng. 117:991–1008.

Hanson, G.J., and K.R. Cook. 1997. Development of excess shear stress parameters for circular jet testing. Pap. 97–2227. Am. Soc. Agric. Eng., St Joseph, MI.

Howard, A.D., and C.F. McLane III. 1988. Erosion of cohesionless sediment by ground water seepage. Water Resour. Res. 24:1659–1674.

Huang, C.H., and J.M. Laflen. 1996. Seepage and soil erosion for a clay loam soil. Soil Sci. Soc. Am. J. 60:408–416.

Iida, T. 2004. Theoretical research on the relationship between return period of rainfall and shallow landslides. Hydrol. Processes 18:739–756.

Iverson, R.M., and J.J. Major. 1986. Groundwater seepage vectors and the potential for hillslope failure and debris flow mobilization. Water Resour. Res. 22:1543–1548.

Jarvis, N.J. 2007. A review of non-equilibrium water flow and solute transport in soil macropores: Principles, controlling factors and consequences for water quality. Eur. J. Soil Sci. 58:523–546.

Jones, J.A.A. 1981. The nature of soil piping: A review of research. Brit. Geomorphol. Res. Group Res. Monogr. Ser. 3. Geobooks, Norwich, UK.

Kemper, W.D., and R.C. Rosenau. 1984. Soil cohesion as affected by time and water content. Soil Sci. Soc. Am. J. 48:1001–1006.

Knapen, A., J. Poesen, G. Govers, G. Gyssels, and J. Nachtergaele. 2007. Resistance of soils to concentrated flow erosion: A review. Earth Sci. Rev. 80:75–109.

Kosugi, K., T. Uchida, and T. Mizuyama. 2004. Numerical calculation of soil pipe flow and its effect on water dynamics in a slope. Hydrol. Processes 18:777–789.

Lamb, M.P., W.E. Dietrich, S.M. Aciego, D.J. DePaolo, and M. Manga. 2008. Formation of Box Canyon, Idaho, by megaflood: Implications for seepage erosion on Earth and Mars. Science 320:1067–1070.

Lamb, M.P., A.D. Howard, W.E. Dietrich, and J.T. Perron. 2007. Formation of amphitheater-headed valleys by waterfall erosion after large scale slumping on Hawaii. Geol. Soc. Am. Bull. 119:805–822.

LaSage, D.M., J.L. Sexton, A. Mukherjee, A.E. Fryar, and S.F. Greb. 2008. Groundwater discharge along a channelized Coastal Plain stream. J. Hydrol. 360:252–264.

Lindow, N., G.A. Fox, and R.O. Evans. 2009. Seepage erosion in layered stream bank material. Earth Surf. Processes Landforms 24: 1693–1701.

Lobkovsky, A.E., B. Jensen, A. Kudrolli, and D.H. Rothman. 2004. Threshold phenomena in erosion driven by subsurface flow. J. Geophys. Res. 109:F04010, doi:10.1029/2004JF000172.

Luo, W., and A.D. Howard. 2008. Computer simulation of the role of groundwater seepage in forming Martian valley networks. J. Geophys. Res. 113:E05002, doi:10.1029/2007JE002981.

McDonnell, J.J. 1990. A rationale for old water discharge through macropores in a steep, humid catchment. Water Resour. Res. 26:2821–2832.

Mickovski, S.B., P.D. Hallett, M.F. Bransby, M.C.R. Davies, R. Sonnenberg, and A.G. Bengough. 2009. Mechanical reinforcement of soil by willow roots: Impacts of root properties and root failure mechanisms. Soil Sci. Soc. Am. J. 73:1276–1285.

Munkholm, L.J., and B.D. Kay. 2002. Effect of water regime on aggregate-tensile strength, rupture energy, and friability. Soil Sci. Soc. Am. J. 66:702–709.

Newman, B.D., B.P. Wilcox, and R.C. Graham. 2004. Snowmelt-driven macropore flow and soil saturation in a semiarid forest. Hydrol. Processes 18:1035–1042.

Nieber, J.L., and G.S. Warner. 1991. Soil pipe contribution to steady subsurface stormflow. Hydrol. Processes 5:329–344.

Nimmo, J.R., and K.S. Perkins. 2002. Aggregate stability and size distribution. p. 317–328. *In* J.H. Dane and G.C. Topp (ed.) Methods of soil analysis. Part 4. SSSA Book Ser. 5. SSSA, Madison, WI.

NRCS. 1997. America's private land: A geography of hope. U.S. Gov. Print. Office, Washington, DC.

Onda, Y., M. Tsujimura, and H. Tabuchi. 2004. The role of subsurface water flow paths on hillslope hydrological processes, landslides and landform development in steep mountains of Japan. Hydrol. Processes 18:637–650.

Owoputi, L.O., and W.J. Stolte. 2001. The role of seepage in erodibility. Hydrol. Processes 15:13–22.

Poesen, J., J. Nachtergaele, G. Verstraeten, and C. Valentin. 2003. Gully erosion and environmental change: Importance and research needs. Catena 50:91–133.

Pollen, N. 2007. Temporal and spatial variability in root reinforcement of streambanks: Accounting for soil shear strength and moisture. Catena 69:197–205.

Pollen, N., and A. Simon. 2005. Estimating the mechanical effects of riparian vegetation on stream bank stability using a fiber bundle model. Water

Resour. Res. 41:W07025, doi:10.1029/2004WR003801.

Reichert, J.M., L.D. Norton, N. Favaretto, C.H. Huang, and E. Blume. 2009. Settling velocity, aggregate stability, and interrill erodibility of soils varying in clay mineralogy. Soil Sci. Soc. Am. J. 73:1369–1377.

Rinaldi, M., and N. Casagli. 1999. Stability of streambanks formed in partially saturated soils and effects of negative pore water pressures: The Siene River (Italy). Geomorphology 26:253–277.

Rinaldi, M., B. Mengoni, L. Luppi, S.E. Darby, and E. Mosselman. 2008. Numerical simulation of hydrodynamics and bank erosion in a river bend. Water Resour. Res. 44:W09428, doi:10.1029/2008WR007008.

Sidle, R.C., and M. Chigira. 2004. Landslides and debris flow strike Kyushu, Japan. Eos Trans. EOS Trans. Am. Geophys. Union 85(15):145–151.

Sidle, R.C., Y. Tsuboyama, S. Noguchi, I. Hosoda, M. Fujieda, and T. Shimizu. 2000. Stormflow generation in steep forested headwater: A linked hydrogeomorphic paradigm. Hydrol. Processes 14:369–385.

Sidle, R.C., A.D. Ziegler, J.N. Negishi, A.R. Nik, R. Siew, and F. Turkelboom. 2006. Erosion processes in steep terrain: Truths, myths, and uncertainties related to forest management in Southeast Asia. For. Ecol. Manage. 224:199–225.

Simon, A., and A.J. Collison. 2002. Quantifying the mechanical and hydrologic effects of riparian vegetation on streambank stability. Earth Surf. Processes Landforms 27:527–546.

Simon, A., A. Curini, S.E. Darby, and E.J. Langendoen. 1999. Streambank mechanics and the role of bank and near-bank processes in incised channels. p. 193–217. *In* S.E. Darby and A. Simon (ed.) Incised river channels. John Wiley & Sons, Chichester, UK.

Simon, A., and S.E. Darby. 1999. The nature and significance of incised river channels. p. 3–18. *In* S.E. Darby and A. Simon (ed.) Incised river channels: Processes, forms, engineering and management. John Wiley & Sons, New York.

Simon, A., N. Pollen-Bankhead, V. Mahacek, and E. Langendoen. 2009. Quantifying reductions of mass-failure frequency and sediment loadings from streambanks using toe protection and other means: Lake Tahoe, United States. J. Am. Water Resour. Assoc. 45:170–186.

Simon, A., and R.R. Wells. 2006. Study of the effects of lateral seepage forces on tension-crack development, bank-failure dimensions, and migration of edge of field gullies. p. 660–666. *In* Proc. Federal Interagency Sediment. Conf., 8th, Reno, NV. 2–6 April 2006. U.S. Gov. Print. Office, Washington, DC.

Thoman, R.W., and S.L. Niezgoda. 2008. Determining erodibility, critical shear stress, and allowable discharge estimates for cohesive channels: Case study in the Powder River basin of Wyoming. J. Hydraul. Eng. 134:1677–1687.

Uchida, T., K. Kosugi, and T. Mizuyama. 2001. Effects of pipeflow on hydrological process and its relation to landslide: A review of pipeflow studies in forested headwater catchments. Hydrol. Processes 15:2151–2174.

Uchida, T., K. Kosugi, and T. Mizuyama. 2002. Effects of pipe flow and bedrock groundwater on runoff generation in a steep headwater catchment in Ashia, central Japan. Water Resour. Res. 38(7):1119, doi:10.1029/2001WR000261.

Ujvari, G., G. Mentes, L. Banyai, J. Kraft, A. Gyimothy, and J. Kovacs. 2009. Evolution of a bank failure along the River Danube at Dunaszekcso, Hungary. Geomorphology 109:197–209.

USEPA. 2000. Atlas of America's polluted waters. EPA 840-B00-002. Office of Water, USEPA, Washington, DC.

van Balen, R.T., C. Kasse, and J. De Moor. 2008. Impact of groundwater flow on meandering: Example from the Geul River, the Netherlands. Earth Surf. Processes Landforms 33:2010–2028.

Vieira, B.C., and N.F. Fernandes. 2004. Landslides in Rio de Janeiro: The role played by variations in soil hydraulic conductivity. Hydrol. Processes 18:791–805.

Wan, C.F., and R. Fell. 2004. Laboratory test on the rate of piping erosion of soils in embankment dams. Geotech. Test. J. 27:295–303.

Weisstein, E.W. 1999. The CRC concise encyclopedia of mathematics. CRC Press, Boca Raton, FL.

Wilson, C., R. Kuhnle, D. Bosch, J. Steiner, P. Starks, M. Tomer, and G.V. Wilson. 2008a. Relative source contributions of eroded sediment to the suspended load of CEAP watersheds in Mississippi, Iowa, Georgia, and Oklahoma. J. Soil Water Conserv. 63:523–532.

Wilson, G.V. 2009. Ephemeral gully erosion by preferential flow through continuous soil-pipes. Earth Surf. Processes Landforms 34:1858–1866.

Wilson, G.V., R.F. Cullum, and M.J.M. Römkens. 2008b. Preferential flow through a discontinuous soil-pipe. Catena 73:98–106.

Wilson, G.V., P.M. Jardine, R.J. Luxmoore, and J.R. Jones. 1990. Hydrology of a forested watershed during storm events. Geoderma 46:119–138.

Wilson, G.V., P.M. Jardine, R.J. Luxmoore, L.W. Zelazny, D.A. Lietzke, and D.E. Todd. 1991a. Hydrogeochemical processes controlling subsurface transport from an upper subcatchment of Walker Branch Watershed during storm events: 1. Hydrologic transport process. J. Hydrol. 123:297–316.

Wilson, G.V., P.M. Jardine, R.J. Luxmoore, L.W. Zelazny, D.E. Todd, and D.A. Lietzke. 1991b. Hydrogeochemical processes controlling subsurface transport from an upper subcatchment of Walker Branch Watershed during storm events: 2. Solute transport processes. J. Hydrol. 123:317–336.

Wilson, G.V., R.K. Periketi, G.A. Fox, S.M. Dabney, F.D. Shields, Jr., and R.F. Cullum. 2007. Seepage erosion properties contributing to streambank failure. Earth Surf. Processes Landforms 32:447–459.

Wu, T.H., R.M. McOmber, R.T. Erbm, and P.E. Beal. 1988. Study of soil–root interaction. J. Geotech. Eng. 114:1351–1375.